

## ONLINE DATA SUPPLEMENT

### Regulatory T cells limit vascular endothelial injury and prevent pulmonary hypertension.

Rasa Tamosiuniene MD PhD<sup>1</sup>, Wen Tian PhD<sup>1</sup>, Gundeep Dhillon MD<sup>3</sup>, Lijuan Wang PhD<sup>1</sup>, Yon K. Sung MD<sup>1</sup>, Lajos Gera PhD<sup>2</sup>, Andrew J. Patterson<sup>3</sup>, Rani Agrawal<sup>3</sup>, Marlene Rabinovitch MD<sup>3</sup>, Kelly Ambler PhD<sup>2</sup>, Carlin S. Long MD<sup>2,4</sup>, Norbert F. Voelkel MD<sup>5</sup>, Mark R. Nicolls MD<sup>1</sup>.

<sup>1</sup>VA Palo Alto Health Care System / Stanford University School of Medicine

<sup>2</sup>University of Colorado Denver School of Medicine

<sup>3</sup>Stanford University School of Medicine

<sup>4</sup>Denver Health

<sup>5</sup>Virginia Commonwealth University

## METHODS

**Echocardiography.** Echocardiographic evaluation of right ventricular dimensions and pulmonary hemodynamics were performed using the Vevo 770 high resolution ultrasound imaging system (VisualSonics, Inc., Toronto, Ontario, Canada) equipped with 25 MHz and 35 MHz transducers. Rats were lightly sedated with isoflurane, volatized with compressed air (3% for induction, 1% for maintenance) for the duration of the procedure. The rats were laid supine on a warmed handling platform and their paws were lightly taped to electrode pads for ECG and respiratory cycle monitoring. Standard left ventricular measurements were made from 2-dimensional-guided M-mode images at the level of the papillary muscles. Pulmonary artery and tricuspid valve Doppler tracings were obtained from separate parasternal short-axis views. The RV free wall and chamber were imaged from a modified parasternal long-axis view. All measurements were made in the expiratory phase of the respiratory cycle. The sonographer was blinded to the study groups during echo acquisition and subsequent analyses.

**Immunohistochemistry and Immunofluorescence imaging.** The left rat lungs were inflated with a 1:1 mixture of OCT and 30% sucrose and were embedded in Tissue Tek OCT (Sakura). A cryostat (HM550) (Microm) was used to cut 7  $\mu$ m cryosections of lung and the sections were placed on superfrost/plus slides (Fisher Scientific). For immunofluorescent staining, the slides were fixed in methanol/acetone (1:1), washed with PBS, incubated in 0.2% Triton (Sigma), and then washed again in PBS. Next, the sections were blocked with normal 10% goat serum and then incubated for 1 h with anti-CD68 (ED-1) (AbD Serotec), anti-CD45RA (OX-33) (AbD Serotec), anti-CD31 (TLD-3A12) (AbD Serotec), anti-rat mast cells (AR32AA4) (BD Pharmingen), anti-BMP2 (G-17) (Santa Cruz Biotechnology), anti-cleaved caspase 3 (Asp175) (Cell Signaling), anti-IL-10 (R&D Systems), anti-FoxP3 (150D/E4) (eBioscience), anti-pSmad2/3 (Ser423/425) (Santa Cruz Biotechnology), anti-TGF- $\beta$ 1 (V) (Santa Cruz Biotechnology), anti-

CD4 (T4/Leu-3) (Abbotec), anti-CD4 (OX-38) (BD Pharmingen), anti-alpha smooth muscle actin (ab5694) (Abcam) and anti-von Willebrand Factor (ab6994) (Abcam) antibodies. Isotype specific antibodies (BD Pharmingen) were used as negative controls. The slides were washed with PBS and then incubated with Alexa Fluor 488 goat anti-mouse IgG, Alexa Fluor 546 donkey anti-goat, Alexa Fluor 647 donkey anti-rabbit, Alexa Fluor 546 donkey anti-rabbit (all Invitrogen), or DyLight 488 donkey anti-mouse (Jackson) conjugated secondary antibodies. TO-PRO-3 (Invitrogen) was used for nuclear staining. The sections were mounted with Vectashield mounting medium (Vector Laboratories). Microscopic analysis was performed with the LSM 510META confocal laser scanning microscope (Carl Zeiss). Integrated fluorescence intensity was used to perform morphometric quantification of the degree of colocalization, expressed as fractional colocalization (value of 1.0 =100% colocalization) measured with ImageJ software. For immunohistochemistry, of CD68, CD45RA, CD31, IL-10, FoxP3, BMPR2, CD4, and cleaved caspase 3, the lung sections were fixed, incubated with blocking serum, and then the primary antibodies listed above. Sections were then either incubated with biotinylated donkey anti-goat or anti-rabbit antibodies (Santa Cruz Biotechnology) or processed with the Animal Research Kit (Dako), followed by streptavidin HRP and diaminobenzidine (Dako). Cells were counted in 10, 400x fields in 4 random sections/animal. Quantification of activated cleaved caspase 3 positive endothelial cells was performed in 4 randomly chosen sections in each experimental group and sixty small pulmonary vessels were analyzed. The percentage of wall thickness was determined using the methodology described by Beppu et al. (2004) and was as follows: % wall thickness =  $(WT1+WT2)/(\text{external diameter of vessel}) \times 100\%$ , where WT1 and WT2 refer to wall thicknesses measured at two points diametrically opposite to each other. The endothelial component of the vessel wall was excluded from the measurements of wall thickness.

**ELISA Analysis.** Commercially available ELISA kits were used to determine serum levels of tumor necrosis factor (TNF) (eBioscience) and interleukin (IL)-6 (Thermo Scientific Pierce).

**Real-time PCR.** For real-time PCR analysis of myocardial gene expression, cardiac tissue was stored in RNALater (Ambion) until RNA was purified with TRIzol reagent (Invitrogen) per product instructions. The RNA concentration was determined using the NanoDrop Spectrophotometer (Thermo Scientific). RNA (1  $\mu\text{g}$ ) was reversed transcribed with the SuperScript III First-Strand Synthesis System to generate cDNA for RT-PCR (Invitrogen). Real-time PCR was performed using the Taqman Gene Expression Assay (Applied Biosystems) and rat cardiac specific primers for each gene (Online Table III). The following genes were assessed:  $\alpha$ - and  $\beta$ -myosin heavy chain (MHC), sarco(endo)plasmic reticulum  $\text{Ca}^{2+}$  ATPase 2a (SERCA2a), atrial natriuretic peptide (ANP), brain natriuretic peptide (BNP), and skeletal  $\alpha$ -actin (SkAct). Each sample was assayed in triplicate (10 ng cDNA/well) and 18S ribosomal RNA was used as an internal control in each well.

**Western Blot Analysis.** Frozen rat lung tissue was homogenized in protein extraction buffer and protease inhibitors (Complete Mini EDTA-free) (Roche) at 4°C. The BCA protein assay (Thermo Scientific Pierce) was used to measure protein concentration. 50  $\mu\text{g}$  protein samples were loaded onto Tris-HCl precast gels with a Mini Protean apparatus (Bio-Rad). Transfer of proteins from the gel to nitrocellulose (Whatman) was performed with the mini transfer apparatus (Bio-Rad). The membranes were blocked for 1 h at room temperature in Odyssey blocking buffer (Li-COR), then incubated overnight at 4°C with anti-BMPR2 (1:500, BD Transduction Laboratories), anti-cleaved caspase 3 (Asp175) (1:1000, Cell Signaling), anti-pSmad2 (Ser465/467) (1:1000, Cell Signaling), anti-smad2 (1:1000, Cell Signaling) and anti- $\beta$  actin (1:5000, AC-15) (Sigma) antibodies. The membranes were washed, incubated with fluorescent IRDye 800CW goat anti-mouse, donkey anti-goat or donkey anti-rabbit secondary antibodies (1:2000, Li-COR) for 1 h, washed again, and then imaged with the Odyssey system

software (Li-COR). For quantification, densitometry of the protein band of interest was divided by the densitometry of the corresponding  $\beta$  actin band using ImageJ software. Reported values were normalized to control group values, which were arbitrarily assigned the value of 1.

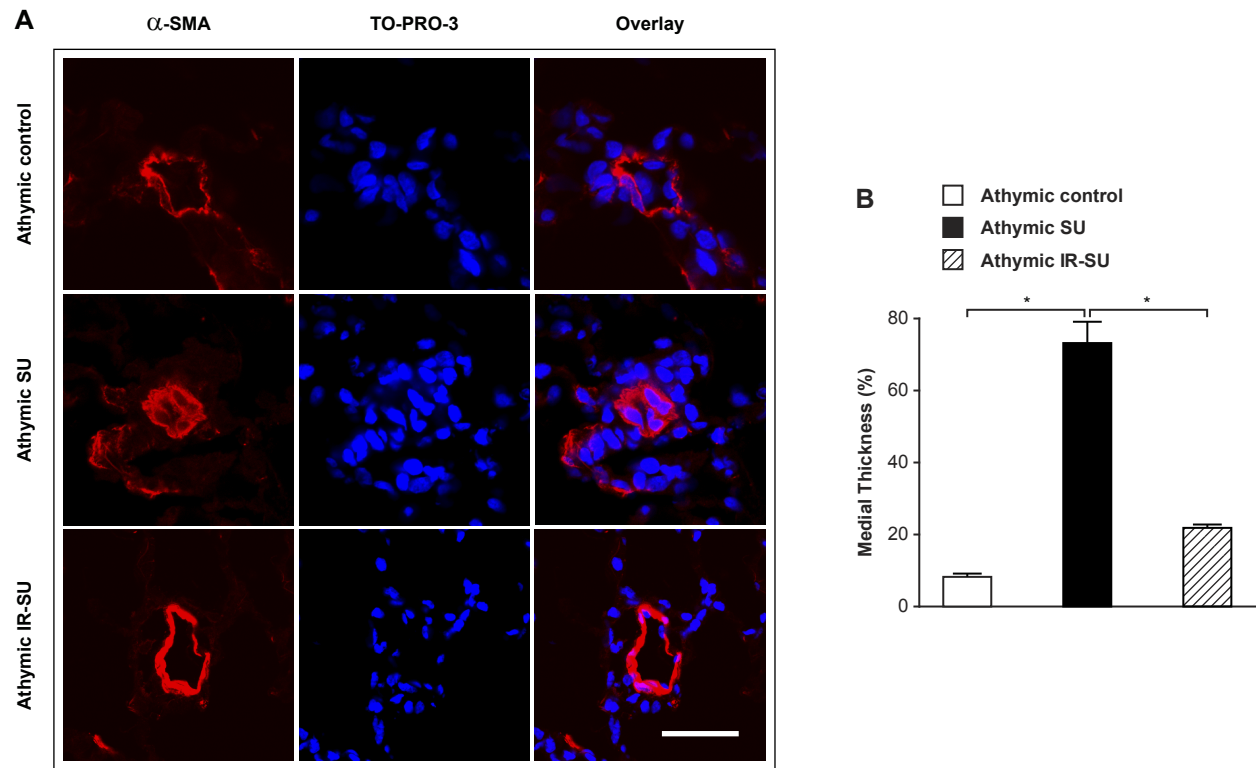
**CD4<sup>+</sup> T cell Depletion.** Monoclonal anti-rat-CD4 antibody, Medical Research Council Oxford (MRC OX) 38 was produced from a hybridoma (Gift of Prof. Bruce Hall, University of New South Wales, Australia). For depletion of CD4<sup>+</sup> T cells, euthymic WAG rats were given i.p injections of anti-CD4 monoclonal antibody (OX-38) at 10 mg/kg on days -1, 0, +1, +2 and weekly thereafter for 3 weeks. As a negative control, rat isotype-matched antibody (mouse IgG2a) (Bio-X-Cell) was injected i.p. in euthymic WAG rats at 10 mg/kg at the same time points.

## **SUPPLEMENT RESULTS**

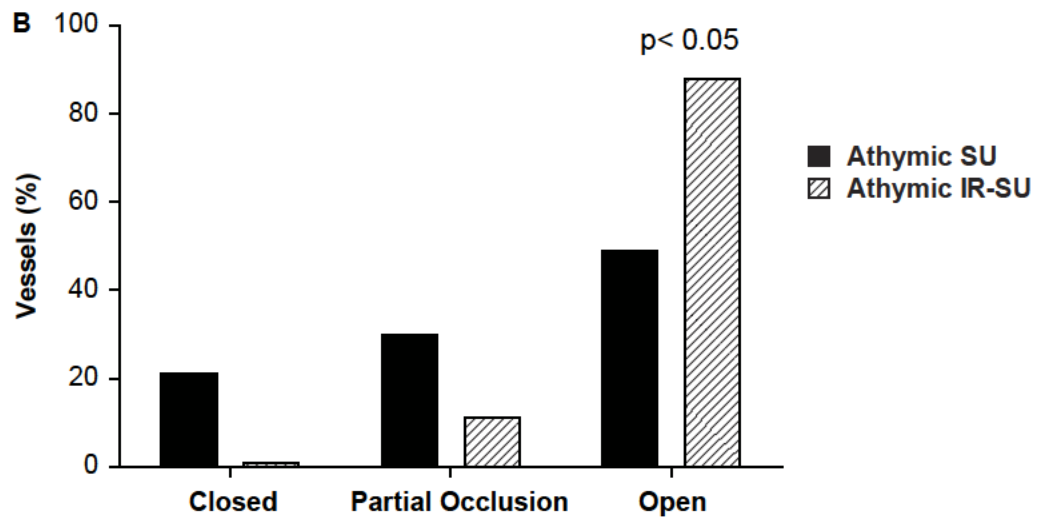
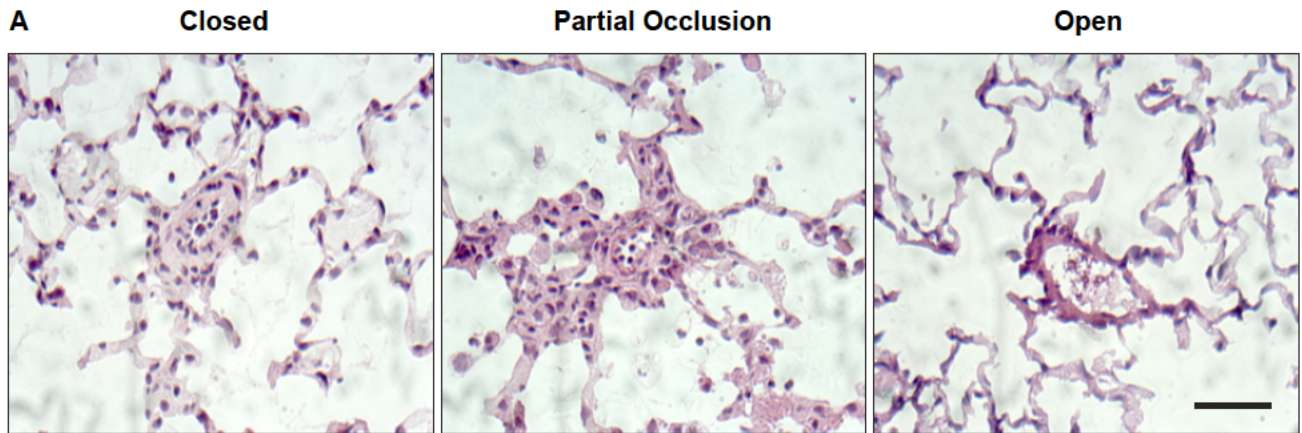
Because pathological left ventricular hypertrophy is characterized by the expression of a signature gene profile which recapitulates embryonic development<sup>1</sup>, we questioned whether the fetal gene program was activated in the RV of the treatment groups. athymic rat RVs were assessed by real-time PCR 21d after SU5416 or vehicle control administration (Online Figure IV). Fetal genes associated with left ventricular stress ( $\beta$ -MHC, skACT, BNP and ANP) were upregulated with PAH whereas adult cardiac muscle-specific genes ( $\alpha$ -MHC and SERCA2a), were decreased with disease. The prevention of PAH by IR also diminished activation of the pathologic fetal gene program. No differential expression of fetal genes was observed in respective left ventricles of these animals (data not shown).

## **SUPPLEMENTAL REFERENCE**

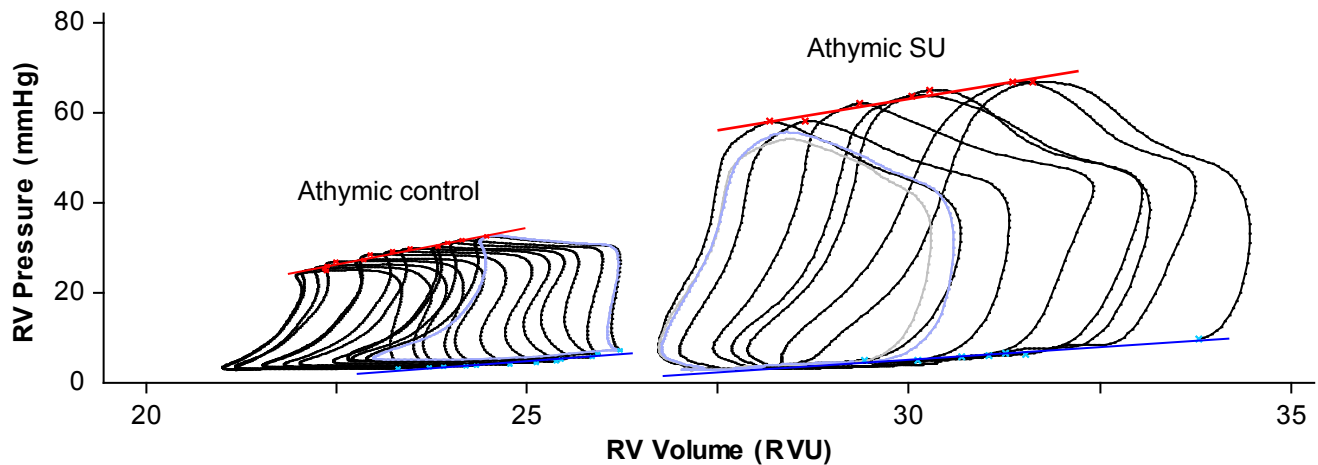
1. Jeong MY, Kinugawa K, Vinson C, Long CS. AFos dissociates cardiac myocyte hypertrophy and expression of the pathological gene program. *Circulation*. 2005;111(13):1645-1651.



**Online Figure I.** IR attenuates medial thickening of precapillary pulmonary vessels. (A) immunofluorescent images of vessels stained with  $\alpha$  smooth muscle actin in lung tissue at d21 (n = 6/group). (B) Percentage of wall thickness of  $\alpha$  smooth muscle actin positive vessels < 100  $\mu$ m in external diameter. Scale bar = 50  $\mu$ m.



**Online Figure II.** IR attenuates occlusion of precapillary pulmonary vessels. (A, B) Hematoxylin and eosin staining of lung sections in athymic SU and athymic IR-SU lung shows totally occluded and partially occluded vessels in lung tissue at d21 (n=4/group).  $p < 0.05$  by chi-square test. Scale bar = 50  $\mu$ m.



**Online Figure III.** Representatives of RV pressure volume loops and RV end-systolic pressure-volume relationships (ESPVR), RV end-diastolic pressure volume relationships (EDPVR) of athymic control and athymic SU rats at d21. Data were obtained during vena cava occlusion. RVU - relative volume units.

**Online Table I.** RV hemodynamic parameters in athymic control, athymic SU and athymic IR-SU rats at d21.

	Athymic control (n=10)	Athymic SU (n=8)	Athymic IR-SU (n=8)
RV-systolic pressure (mmHg)	25.78 ± 9.52	71.66 ± 11.69*	36.63 ± 6.81
dP/dt max (mmHg/s)	945.5 ± 92.5	3089 ± 1000*	1583 ± 576.7

dP/dt max, maximal rate of pressure increase.

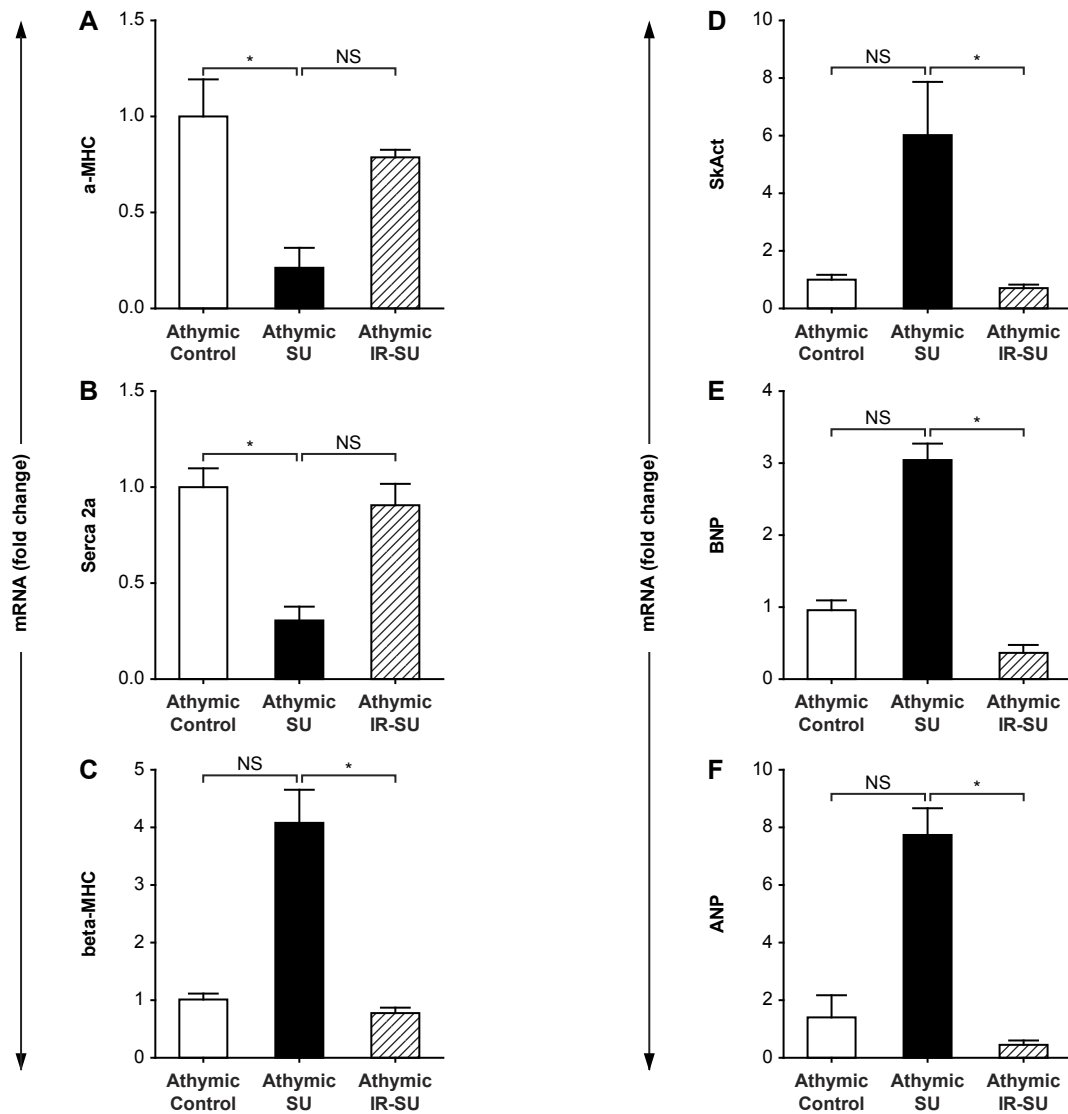
Values are means ± SEM. \*p<0.05 vs athymic controls&athymic SU, vs athymic SU&athymic IR-SU.

**Online Table II.** RV and LV hemodynamic parameters in athymic control and athymic SU rats at d21.

	Athymic control (n=12)	Athymic SU (n=15)
mPAP (mmHg)	20.52 ± 11.82	65.31 ± 7.7*
LVEDP (mmHg)	7.15 ± 4.71	7.37 ± 6.43
RVEDP (mmHg)	4.8 ± 2.81	9.10 ± 4.39*
RV ESPVR (mmHg/RVU)	2.63 ± 1.77	5.23 ± 3.38
RV EDPVR (mmHg/RVU)	0.51 ± 0.51	0.98 ± 1.39

mPAP, mean pulmonary artery pressure; L(R)VEDP, left (right) ventricular end-diastolic pressure, RV ES(D)PVR, right ventricular end-systolic (diastolic) pressure volume relations.

Values are means ± SEM. \*p<0.05 vs athymic controls.

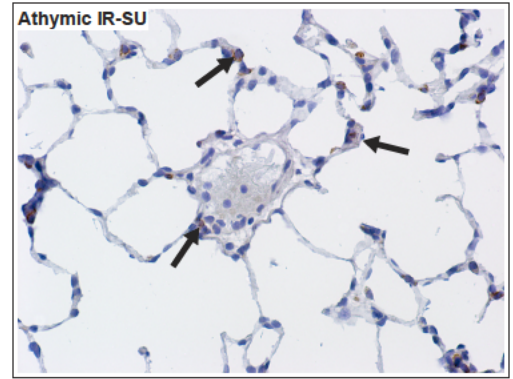
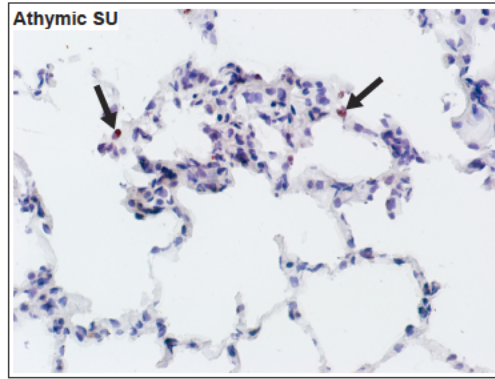
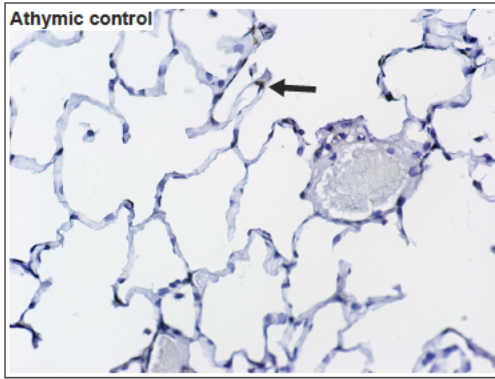


**Online Figure IV.** IR of athymic rats prevents activation of the pathological fetal gene program. (A-F) Real-time PCR of RV myocardial tissue for detection of non-pathologic  $\alpha$ -MHC and SERCA2a fetal genes along with pathologic  $\beta$ -MHC, SkAct, BNP and ANP fetal genes at d21. Results are expressed as arbitrary units (AU) and fold change after normalization for 18S. The AU was set as the average value of the control group (n=4/group). Data are shown as means with error bars representing SEM. \* p<0.05.

**Online Table III.** Sequence of the primers used for the RT-PCR reaction.

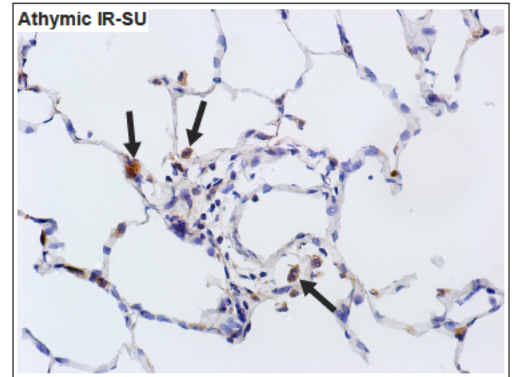
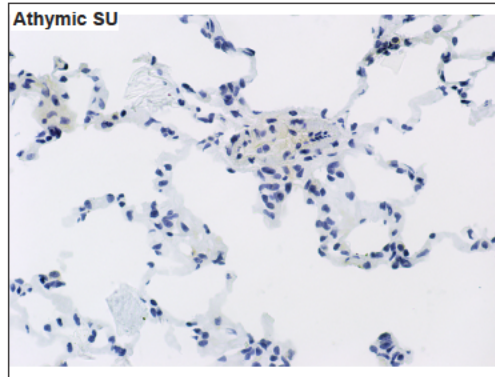
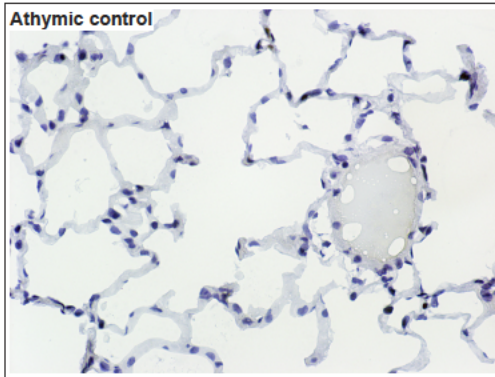
Primer	Sequence
a-MHC F	CCTGTCCAGCAGAAAGAGC
a-MHC R	CAGGCAAAGTCAAGCATTTCATTTATTGTG
18S F	GCCGCTAGAGGTGAAATTCCTG
18S R	CTTTCGCTCTGGTCCGTCTT
BNP F	GGTGCTGCCCCAGATGATT
BNP R	CTGGAGACTGGCTAGGACTTC
Serca 2a F	GGCCAGATCGCGCTACA
Serca 2a R	GGCCAATTAGAGAGCAGGTTT
SkAct F	CCACCTACAACAGCATCATGAAGT
SkAct R	GACATGACGTTGTTGGCGTACA
beta-MHC F	CGCTCAGTCATGGCGGAT
beta-MHC R	GCCCCAATGCAGCCAT
ANP F	GCGAAGGTCAAGCTGCTT
ANP R	CTGGGCTCCAATCCTGTCAAT

All primers are presented in a 5'-3' orientation.

**A**CD4<sup>+</sup>

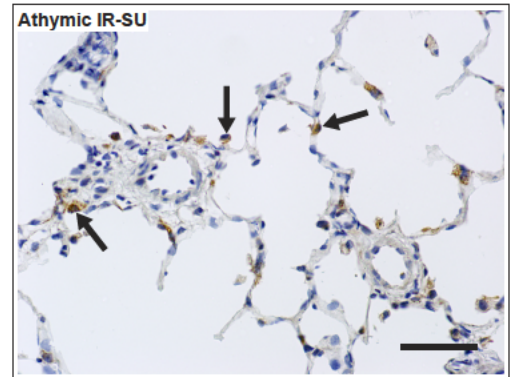
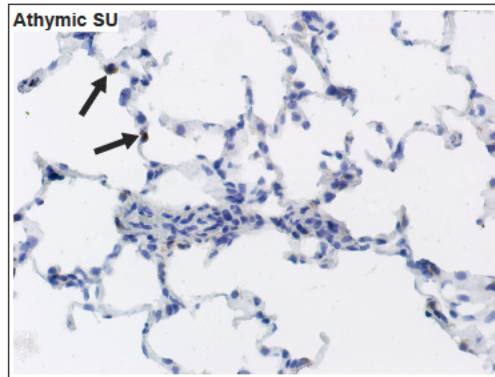
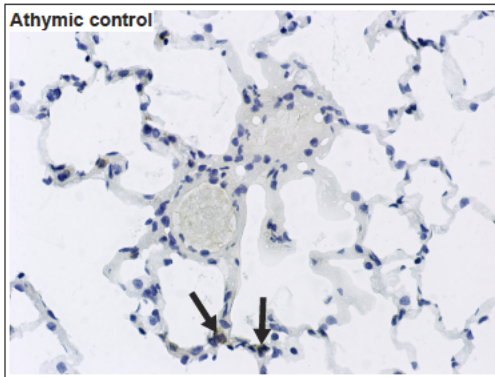
CD4 <sup>+</sup> cells	Group	Quantity / High power field
	Athymic control	1.25 ± 0.25
	Athymic SU	1.57 ± 0.85
	Athymic IR-SU	12.58 ± 7.07*

\* p&lt;0.05 vs athymic SU&amp;athymic IR-SU group

**B**FoxP3<sup>+</sup>

FoxP3 <sup>+</sup> cells	Group	Quantity / High power field
	Athymic control	0.0 ± 0.0
	Athymic SU	0.0 ± 0.0
	Athymic IR-SU	7.08 ± 2.05*

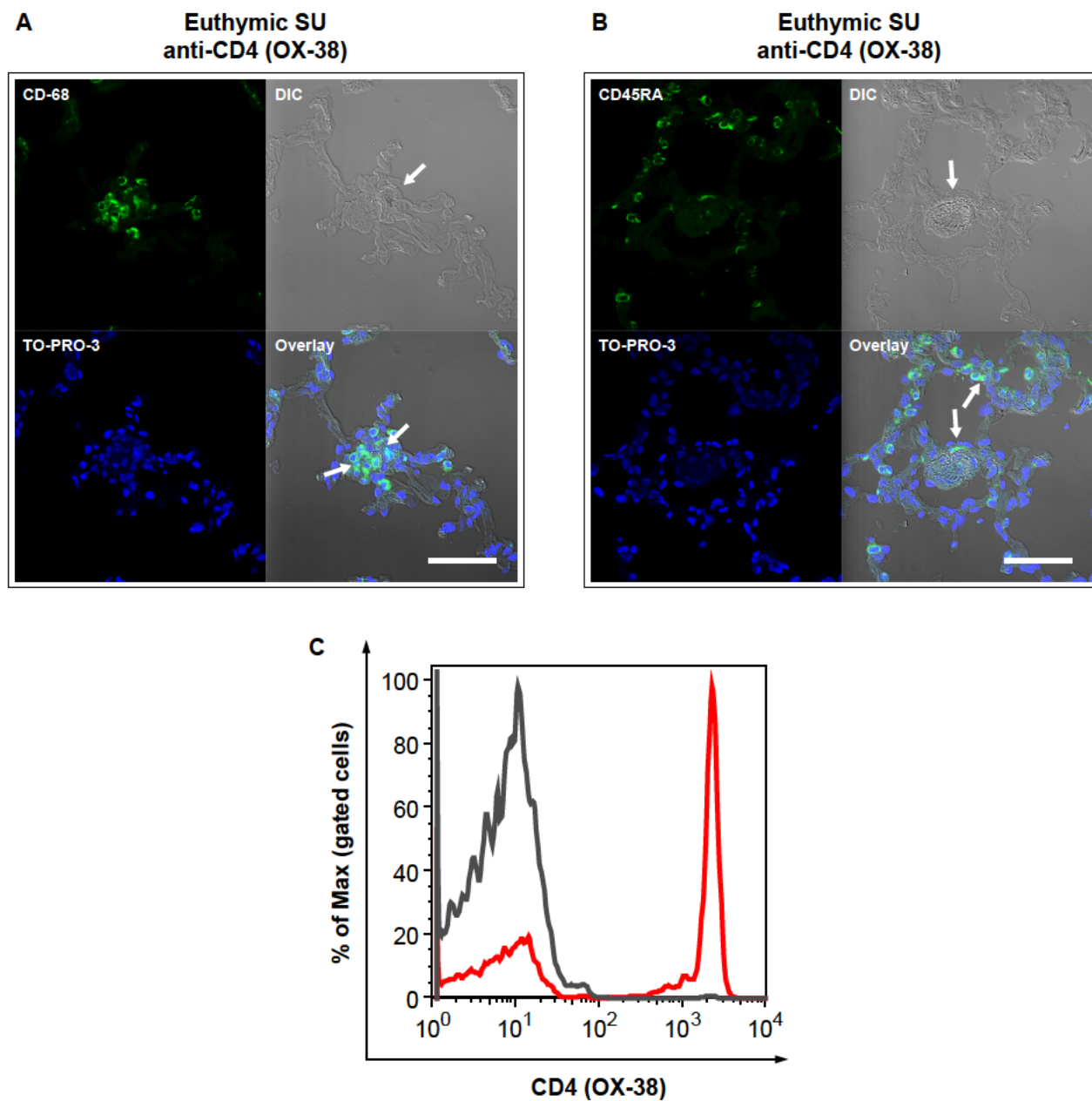
\* p&lt;0.05 vs athymic SU&amp;athymic IR-SU group

**C**IL-10<sup>+</sup>

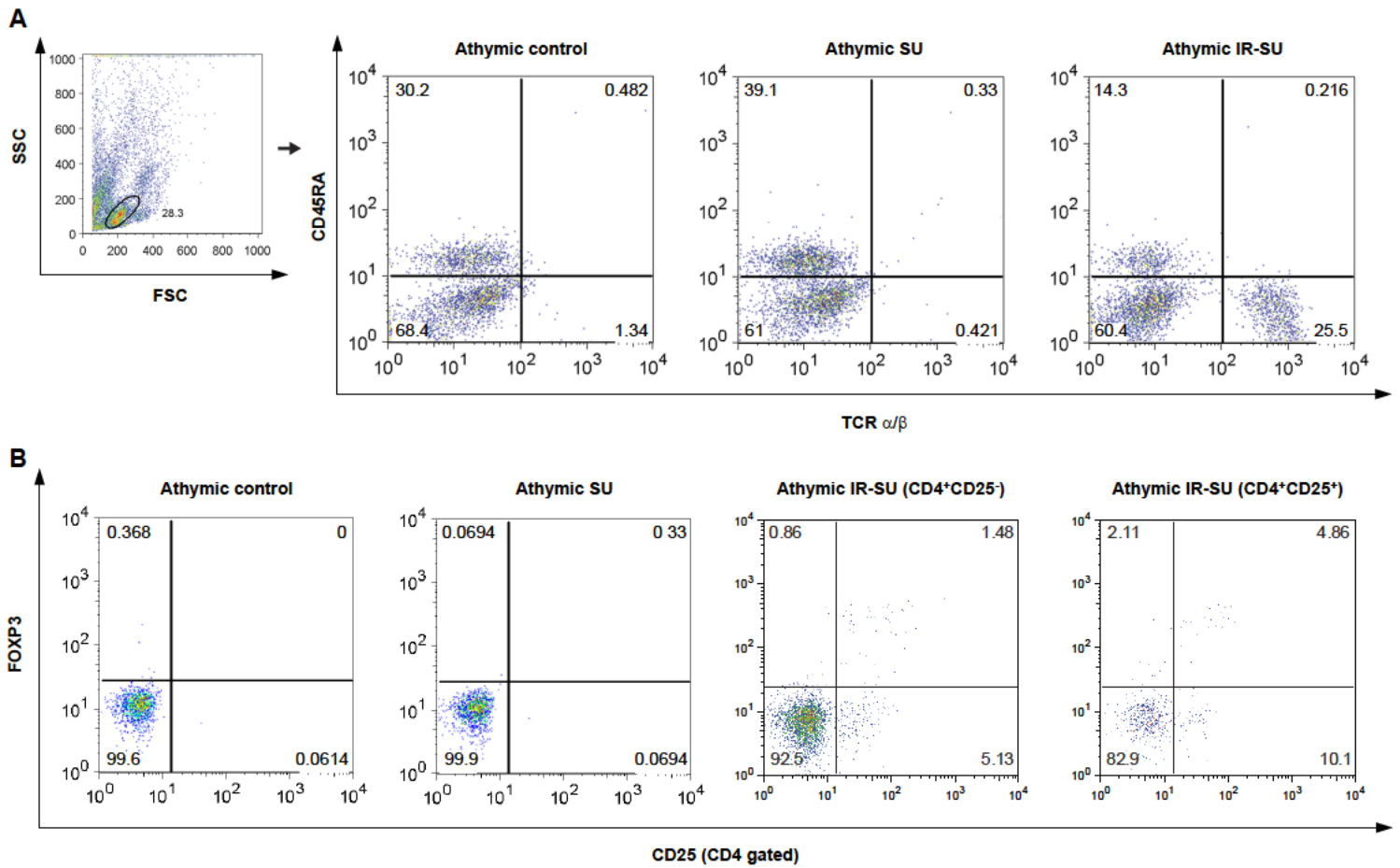
IL-10 <sup>+</sup> cells	Group	Quantity / High power field
	Athymic control	2.15 ± 0.75
	Athymic SU	2.87 ± 1.48
	Athymic IR-SU	11.08 ± 5.05*

\* p&lt;0.05 vs athymic SU&amp;athymic IR-SU group

**Online Figure V.** IR of athymic rats leads to increased infiltration of CD4<sup>+</sup>, FoxP3<sup>+</sup>, IL-10<sup>+</sup> cells in the perivascular regions of lungs. (A, B, C) Immunohistochemistry and quantification for expression of CD4<sup>+</sup>, FoxP3<sup>+</sup>, IL-10<sup>+</sup> cells (arrows) in lungs on d21 of athymic control, athymic SU and athymic IR-SU animals (n = 4/group). Data are shown as means with SEM. \* p<0.05. Scale bar = 50 μm.



**Online Figure VI.** Evidence of perivascular inflammation and occlusion of small pulmonary vessels in lungs of euthymic SU rats after CD4 depletion. (A, B) Green immunofluorescent images for macrophages (arrows) stained with CD68 and B cells (arrows) stained with CD45RA in euthymic rats at d21 after anti-CD4 administration. Differential interference contrast (DIC) histology demonstrates occluded vessels (arrow) in lungs of euthymic SU animals after CD4 depletion (n=4/group). (C) Fluorescence histogram from flow cytometry for CD4 (OX-38) detection on peripheral blood of euthymic SU isotype control (red line) and euthymic SU rats after CD4 depletion (black line) at d21 after anti-CD4 administration (n=4/group). Scale bars=50  $\mu$ m.



**Online Figure VII.** Confirmation of putative Tregs (CD4<sup>+</sup>CD25<sup>hi</sup>FoxP3<sup>+</sup>) cells by flow cytometry in the peripheral blood within 21days after IR. (A) Flow cytometry data of peripheral blood for TCR $\alpha/\beta$  and CD45RA detection on d7 in athymic controls, athymic SU, and athymic IR-SU. (n = 4/group). (B) Flow cytometry data for Tregs (CD4<sup>+</sup>CD25<sup>hi</sup>FoxP3<sup>+</sup> cells) detection in the peripheral blood in athymic control, athymic SU, athymic IR-SU (CD4<sup>+</sup>CD25<sup>-</sup>) and athymic IR-SU (CD4<sup>+</sup>CD25<sup>+</sup>) on d21 (n = 8/group).